Ocean Dynamics (2019) 69:1121–1132
https://doi.org/10.1007/s10236-019-01290-2

Normal modes and resonance in Ontario Lacus: a hydrocarbon lake of Titan

David Vincent[1] · **Jonathan Lambrechts**[1] · **Özgür Karatekin**[2] · **Tim Van Hoolst**[2] · **Robert H. Tyler**[3] · **Véronique Dehant**[2,4] · **Eric Deleersnijder**[5,6]

Received: 11 April 2019 / Accepted: 15 July 2019 / Published online: 31 August 2019

Abstract

The natural modes of Ontario Lacus surface oscillations, the largest lake in Titan's southern hemisphere, are simulated and analyzed as they are potentially of broad interest in a variety of dynamical researches. We found that tidal forces are too low in frequency to excite the (barotropic) normal modes. Broadband wind forcing likely spans the resonant frequencies. High wind speed, which could be encountered under episodic phenomena such as storms, would be required to significantly excite the normal modes. While the slower baroclinic normal modes could more easily be resonantly forced by the low-frequency tidal forces, addressing this issue demands unavailable information about the lake stratification.

Keywords Ontario Lacus · Natural modes · Titan · Extraterrestrial oceanography

1 Introduction

Titan, the largest moon of Saturn, is known for its surface lakes and seas filled with liquid hydrocarbons. The Cassini spacecraft, which had been investigating the Saturnian system from 2004 to 2017, detected a methane cycle similar to the hydrological cycle on Earth (Atreya et al. 2006) as well as surface lakes and seas filled with liquid hydrocarbons (mainly methane and ethane) (Stofan et al. 2007; Brown et al. 2008; Cordier et al. 2009). The distribution of these lakes and seas is asymmetric with respect to the equator (Aharonson et al. 2009): there are more lakes in the northern hemisphere, where the largest liquid bodies are located (Hayes et al. 2008, 2018). The present work focuses on the largest lake of the southern hemisphere, Ontario Lacus. It is centered at 72° S and 176° E and covers approximately an area of 200 km × 70 km (Wall et al. 2010). It exhibits well-documented shoreline variations: Turtle et al. (2011) suggested that the difference between the ISS[1] images taken in 2005 (on June 6, Rev09, $L_s = 306°$)[2] and 2009 (on March 27, T51, $L_s = 355°$) corresponds to possible shoreline variations. This assumption was given additional support by synthetic aperture radar (SAR) images in 2009 (T57, $L_s = 358°$ and T58, $L_s = 359°$) (Wall et al. 2010; Hayes et al. 2011).

Various attempts have been made to understand and explain these variations. Tides were ruled out by Vincent et al. (2016) as the tidal range is too small. Nowadays, the most common explanation involves evaporation/infiltration of surface liquid (Turtle et al. 2011; Lunine et al. 2009) as the observations took place during the southern summer, when

Responsible Editor: Pierre F.J. Lermusiaux

✉ David Vincent
david.vincent@uclouvain.be

[1] Institute of Mechanics, Materials and Civil Engineering (IMMC), Université catholique de Louvain, Avenue Georges Lemaître 4-6 bte L4.05.02, 1348 Louvain-la-Neuve, Belgium

[2] Royal Observatory of Belgium, 3 Avenue Circulaire, 1180 Bruxelles, Belgium

[3] Department of Astronomy, University of Maryland, College Park, MD 20742-2421, USA

[4] Earth and Life Institute (ELI), Université catholique de Louvain, 2 Croix du Sud, 1348 Louvain-la-Neuve, Belgium

[5] Institute of Mechanics, Materials and Civil Engineering (IMMC) & Earth and Life Institute (ELI), Université catholique de Louvain, 4 Avenue Georges Lemaître, B-1348 Louvain-la-Neuve, Belgium

[6] Delft Institute of Applied Mathematics (DIAM), Delft University of Technology, Van Mourik Broekmanweg 6, 2628 XE Delft, The Netherlands

[1] Imaging Science Subsystem: it takes pictures in visible, near-ultraviolet, and near-infrared light (see Porco et al. 2004).

[2] The solar longitude of Saturn, L_s, is the angle between the sun and Saturn and describes the season of Saturn and its moons.

evaporation was predicted to be the largest. Due to their low resolution, analysis of ISS images was inconclusive and the existence of seasonal shoreline variations remained questionable as the data are, within measurement error, consistent with no changes at all (Cornet et al. 2012). Subsequent SAR images (T65 in 2010, $L_s = 5.5°$) suggested no significant shoreline changes in comparison with 2009 images. On the other hand, lacustrine features of the southern hemisphere seem to disappear between subsequent SAR observations (from 2007 to 2008/2009), corresponding to liquid evaporation or infiltration into the ground (Hayes et al. 2011, 2016). Such observations tilt the balance in favor of shoreline variations taking place in Titan southern hemisphere (at least from 2007 to 2009). Ontario Lacus would likely experience such variations although they could be less significant than suggested by the variations observed between 2005 ISS and 2009 SAR images.

While the tidal motion of Titan's liquid bodies has been the subject of several studies (see Tokano 2010; Tokano et al. 2014; Vincent et al. 2016, 2018), the normal modes were only briefly investigated by Lorenz (1994), Dermott and Sagan (1995), and Tokano (2010). Dermott and Sagan (1995) used Merian's formula to investigate resonance phenomenon in a hypothetical rectangular lake on Titan, while Tokano (2010) calculated the period of a fundamental slosh in Ontario Lacus and Kraken Mare. Such modes need to be understood for a whole range of dynamical studies. Furthermore, they could form a signature that could be remotely sensed and, if they were observed, could possibly be used to infer lake characteristics such as the bathymetry. Indeed, detecting liquid motion associated with a natural period of the lake could give further insight into the bathymetry as the natural periods are related to the depth of the lake. Using such an inverse approach, one could, for instance, gain an insight about the material/configuration properties of a wind chime from the modes excited by broadband wind.

The resonant frequencies of barotropic modes[3] of a lake with complex shoreline and bathymetry such as Ontario Lacus can be bound by considering its geometry. The highest resonant frequencies would take place in a small cove, where a high-frequency slosh could occur. One can obtain a simple estimate of the lower bound from the period of a fundamental slosh[4] along the larger axis of the lake, of length L. This period is approximated by Merian's formula (Merian 1828) for a rectangular domain: $T = \frac{2L}{\sqrt{gh}}$, where $g = 1.352$ m/s^2 is the mean gravitational acceleration and h is the mean depth of the lake. For Ontario Lacus, it results in a period much smaller than 1 Titan day (TD). Such modes could not be excited in the models of Tokano (2010) and Vincent et al. (2016) as the only forcing taken into account was that induced by the orbital eccentricity and Titan's obliquity, whose period is 1 TD. Other astronomical forcings with smaller magnitude that were not taken into account in previous studies or some atmospheric forcings could have a period matching those of the barotropic normal modes. Baroclinic modes could also resonate and generate significant liquid displacement within the lake but are not associated with large surface elevations. Furthermore, there is not enough information about the stratification of Ontario Lacus to study them properly; therefore, we did not consider these modes.

We numerically studied the normal modes of Ontario Lacus for two bathymetries available in the literature, that of Ventura et al. (2012) and that of Hayes (2016) and Mastrogiuseppe et al. (2018).[5] The bathymetries were derived from different data sets and using different methods. Ventura et al. (2012) used a model to derive the bathymetry from the SAR data of the T65 flyby (January 12, 2010) while Hayes (2016) and Mastrogiuseppe et al. (2018) derived their bathymetry from the T49 flyby (December 21, 2008) by means of an extrapolation method. The methodology of Ventura et al. (2012) is a combination of electromagnetic modeling and a Bayesian approach to perform the inversion and to derive from SAR backscattering values the lake optical thickness. The conversion to physical depth is then achieved by using the loss tangent value as calculated in Hayes et al. (2010). Hayes (2016) and Mastrogiuseppe et al. (2018) applied the method of Mastrogiuseppe et al. (2014) to the altimetry data from T49. This method consists in deriving the bathymetry from subsurface reflections in the Cassini radar altimeter. Nevertheless, T49 was the first pass over a liquid body and the default attenuator settings were overwhelmed, leading to saturation. Mastrogiuseppe et al. (2016, 2018) used a radar altimetry simulator to recover the data over the saturated area, resulting in the bathymetry reported in Hayes (2016). A more detailed comparison of the methods is available in Section 2.3 of Vincent et al. (2016) while technical details are available in Ventura et al. (2012) and Mastrogiuseppe et al. (2014, 2016, 2018). The lake shoreline considered are derived from T58/T59 flyby. It corresponds to the lowest level of the lake (see Fig. 1[6]). Due

[3]The former concern the motion of a constant density liquid and are mostly external modes, i.e. approximately depth-dependent, while the latter differently impacts each layer of various density, resulting in internal oscillations.

[4]A fundamental slosh is a normal mode with 1 node in the domain, i.e. it is the longest standing wave that can be observed in the domain.

[5]Although the bathymetry was derived following the method described in Mastrogiuseppe et al. (2018), it was first published in Hayes (2016). We refer to this bathymetry as the bathymetry of Hayes (2016) throughout this article.

[6]Reprinted from *Transient surface liquid in Titan's polar regions from Cassini*, 211, Hayes, A. G.; Aharonson, O.; Lunine, J. I.; Kirk, R. L.; Zebker, H. A.; Wye, L. C.; Lorenz, R. D.; Turtle, E. P.;

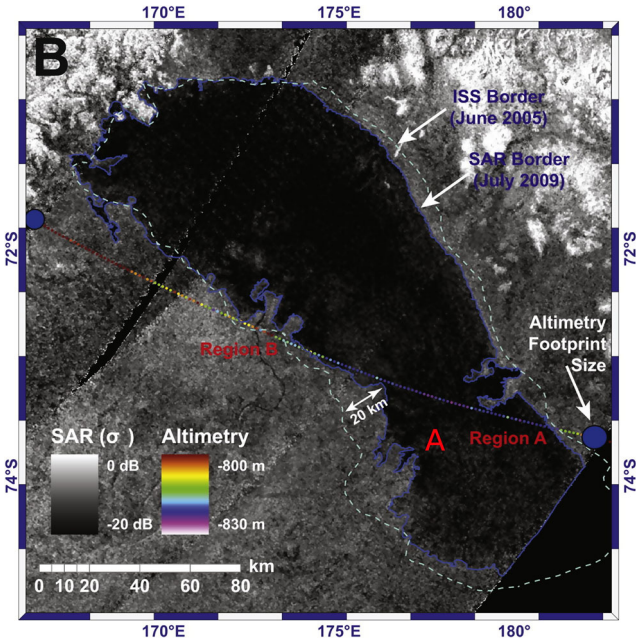

Fig. 1 Synthetic aperture radar map of Ontario Lacus. The dashed line corresponds to the ISS shorelines from 2005. The red letter A denotes the area where the largest shoreline variations occurred (adapted from Hayes et al. 2011; original image credit: Cassini Radar Science team, NASA/JPL/Caltech)

to the complexity of Ontario Lacus' shoreline, unstructured grids are used to discretize the domain. It allows for a better representation of the shoreline without significantly increasing the computational and memory costs. The article is organized as follows: the method used to simulate the natural modes and periods of the lake is presented in Section 2. The periods of the various astronomical forcings acting on Titan are discussed in Section 3 and compared with the natural periods of Ontario Lacus in Section 4. Among the natural modes predicted, some of them stand out as they correspond to large area(s) with positive/negative sea surface elevation and could therefore be detected by an orbiter. They are briefly introduced in the same section. Finally, the results are discussed in Section 5 and conclusions are drawn in Section 6.

2 Method

A normal mode (also called eigenmode) is a pattern of motion under which a system can freely oscillate following a perturbation of its equilibrium state. The frequency associated with the oscillation is called the normal frequency. The normal modes of a linear system form a complete basis set, i.e. any motion of the system can be described as a weighted sum of its eigenmodes. The motion associated with the excitation of a normal mode of a liquid body is called a seiche, which is defined by Baretta-Bekker et al. (1998) as "a standing wave occurring in lakes or semi-enclosed embayments as a result of some sudden disturbance." The topography of the basin determines the form and period of the different seiche modes that may occur. These modes can be predicted from the linearized equations of motion.

Various methods allowing computing the eigenmodes of a liquid domain are described hereafter. For regular structured grids, the eigenmodes can be computed analytically by introducing a space Fourier mode in the discretized equations, leading to the dispersion relation which depends on the grid and numerical scheme (e.g. Sauter and Wittum 1992). Another way to study the eigenmodes is to solve the stationary equations[7] for a range of angular frequencies (e.g. Webb 2013). This allows predicting the frequencies associated with resonance (and, hence, the normal periods and normal modes). Ontario Lacus has a complex shoreline and bathymetry which would require a high-resolution structured grid to be properly captured. On the other hand, the geometrical flexibility of unstructured meshes allows one to locally increase the spatial resolution. This permits an accurate representation of the shoreline and the bathymetry (see Fig. 2) while demanding less memory and computer time than calculations based on a structured mesh. The abovementioned approaches being not easily applicable to unstructured grids, we used the alternative approach of Bernard et al. (2008), which is adapted to these grids. The key features of this method are laid out below. The modes are predicted from the linearized, frictionless shallow water equations:

$$\begin{cases} \dfrac{\partial \boldsymbol{u}}{\partial t} + f\boldsymbol{e}_z \wedge \boldsymbol{u} + g\nabla\eta = 0 \\ \dfrac{\partial \eta}{\partial t} + \nabla\cdot(h\boldsymbol{u}) = 0 \end{cases} \tag{1}$$

where $\boldsymbol{u}$ is the depth-averaged velocity, ∇ is the horizontal del operator, $f = 2\Omega\sin\phi$ is the Coriolis parameter ($\Omega = 4.5601\times10^{-6}$ s^{-1} is Titan's orbital angular velocity and ϕ is the latitude), $\boldsymbol{e}_z$ is a unit vector pointing upwards in the local non-inertial Cartesian basis, $g = 1.352$ m/s^2 is the mean gravitational acceleration at Titan's surface, η is the surface elevation (positive upward), and h is the reference height of the liquid column.

One can rewrite this system as

$$\frac{\partial \mathbf{U}}{\partial t} + \nabla\cdot\mathbf{F}(\mathbf{U}) + \mathbf{S}(\mathbf{U}) = \mathbf{0} \tag{2}$$

Paillou, Philippe; Mitri, G and others, 655–671, Copyright (2011), with permission from Elsevier

[7] These equations are obtained by separation of variables.

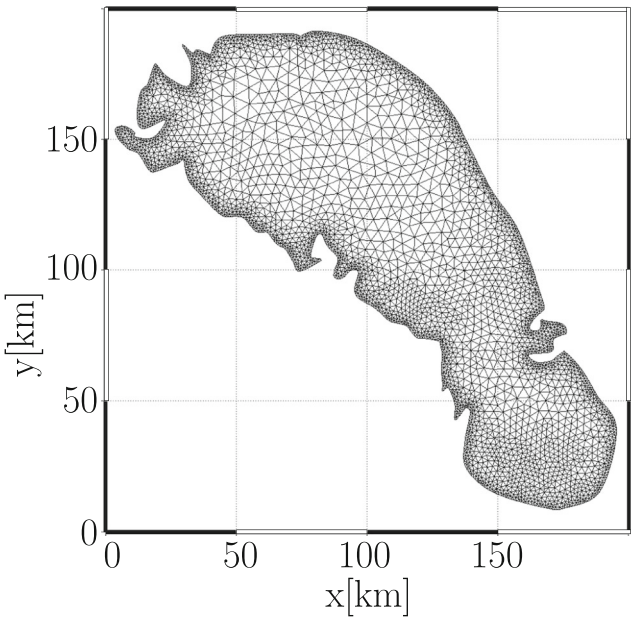

Fig. 2 Discretization of Ontario Lacus using mesh generation package GMSH (see Geuzaine and Remacle 2009, http://geuz.org/gmsh/). The mesh is refined nearshore and where the bathymetry gradient is significant

where $\mathbf{U} = \begin{pmatrix} \eta \\ u \\ v \end{pmatrix}$ is the vector of unknowns, $\mathbf{F} = \begin{pmatrix} hu & hv \\ g\eta & 0 \\ 0 & g\eta \end{pmatrix}$ is the flux matrix, and $\mathbf{S} = \begin{pmatrix} 0 \\ -fv \\ fu \end{pmatrix}$ is a vector related to the Coriolis force. These equations are discretized on an unstructured mesh following the discontinuous Galerkin finite element method (DGFEM): Eq. 2 is multiplied by a test function and integrated over the domain. Using a Riemann solver to compute the flux at the element interfaces, one obtains the semi-discrete discontinuous Galerkin (DG) formulation for a spatial piecewise discontinuous polynomial approximation $\mathbf{U}^p$

$$\frac{\partial \mathbf{U}^p}{\partial t} = \mathbf{L}\mathbf{U}^p \tag{3}$$

where $\mathbf{L}$ is the DG formulation of the linear shallow water space operator (see Bernard et al. 2008 for further details about this transformation). Finally, this linear operator transforms to

$$\frac{\partial}{\partial t}\mathbf{U}^p = \mathbf{M}^{-1}\mathbf{A}\mathbf{U}^p \tag{4}$$

where $\mathbf{M}$ is the mass matrix of the domain[8] and $\mathbf{A}$ is a matrix representing the spatial terms. $\mathbf{M}^{-1}\mathbf{A}$ is never assembled numerically as it would require a time- and resource-consuming inversion of $\mathbf{M}$. Consequently, the linear operator corresponding to the numerical equation is

$$\mathbf{M}\frac{\partial}{\partial t}\mathbf{U}^p = \mathbf{A}\mathbf{U}^p \tag{5}$$

This is a generalized eigenvalue problem whose complex eigenvalues, λ, satisfy the fact that $\mathbf{A} - \lambda\mathbf{M}$ is singular (i.e. the determinant is zero). The discrete solutions $\mathbf{U}^p$ are the real part of

$$\mathbf{U}^p = \mathrm{Re}\{\mathbf{X}^p(x, y)e^{j\lambda t}\} \tag{6}$$

where $\mathbf{X}^p(x, y)$ is the eigenvector and $j = \sqrt{-1}$. These eigenvalues and the associated eigenvectors $\mathbf{X}^p$ can be computed using `eig` function of the `scipy.linalg` package of the python library (see Jones et al. 2001). Indeed, this is cheaper than inverting $\mathbf{M}$ and then multiplying $\mathbf{A}$ by $\mathbf{M}^{-1}$. Function `eig` uses the `ggev` routine from LAPACK and BLAS libraries. This routine performs a QZ decomposition (also called generalized Schur decomposition) to compute the eigenvalues and eigenvectors.

The eigenvalues should be purely imaginary as no dissipation term is present in Eq. 1. However, they are actually complex (see Fig. 3). This is due to the dissipation introduced in the discrete equations by the Riemann solver used to deal with the spatial operators (Bernard et al. 2008). The real part of the eigenvalues quantifies this dissipation. For this application, the real part of the eigenvalues ranges from 0 to 0.03 s^{-1} or 0.04 s^{-1}, depending on the bathymetry. The eigenmodes of interest in our analysis (they are represented by red dots on Fig. 3) correspond to eigenvalues whose real part is small (it is at most $\mathcal{O}(10^{-8})$ s^{-1}). The real parts of some eigenvalues are much more significant, but they are associated with modes corresponding to numerical dissipation (i.e. without any physical meaning). The eigenvalues always come in complex conjugate pairs of same norms and dissipation. Furthermore, they are characterized by the same frequency but with opposed directions of rotation. As the eigenvalues are complex, so are the eigenvectors. Both real and imaginary parts contribute to the motion associated with the eigenmode. Indeed, eigenmode theory relies on the assumption that the solutions are periodic , i.e. $\mathbf{U}^p(x, y, t) = \mathrm{Re}\{\mathbf{X}^p(x, y)e^{j\omega t}\}$, where $j = \sqrt{-1}$, ω is the imaginary part of the eigenvalues, and $\mathbf{X}^p(x, y) = \mathbf{X}^p_{\mathrm{r}}(x, y) + j\mathbf{X}^p_{\mathrm{i}}(x, y)$ are the eigenvectors – $\mathbf{X}_{\mathrm{r}}$ and $\mathbf{X}_{\mathrm{i}}$ respectively denoting the real and imaginary parts of the eigenvectors. For complex eigenvectors, the solution can be rewritten as

$$\mathbf{U}^p(x, y, t) = \mathrm{Re}\left\{\left[\mathbf{X}^p_{\mathrm{r}}(x, y) + j\mathbf{X}^p_{\mathrm{i}}(x, y)\right] [\cos(\omega t) + j\sin(\omega t)]\right\} \tag{7}$$

[8] The mass matrix results from the integral of the product of the shape functions over each element of the domain.

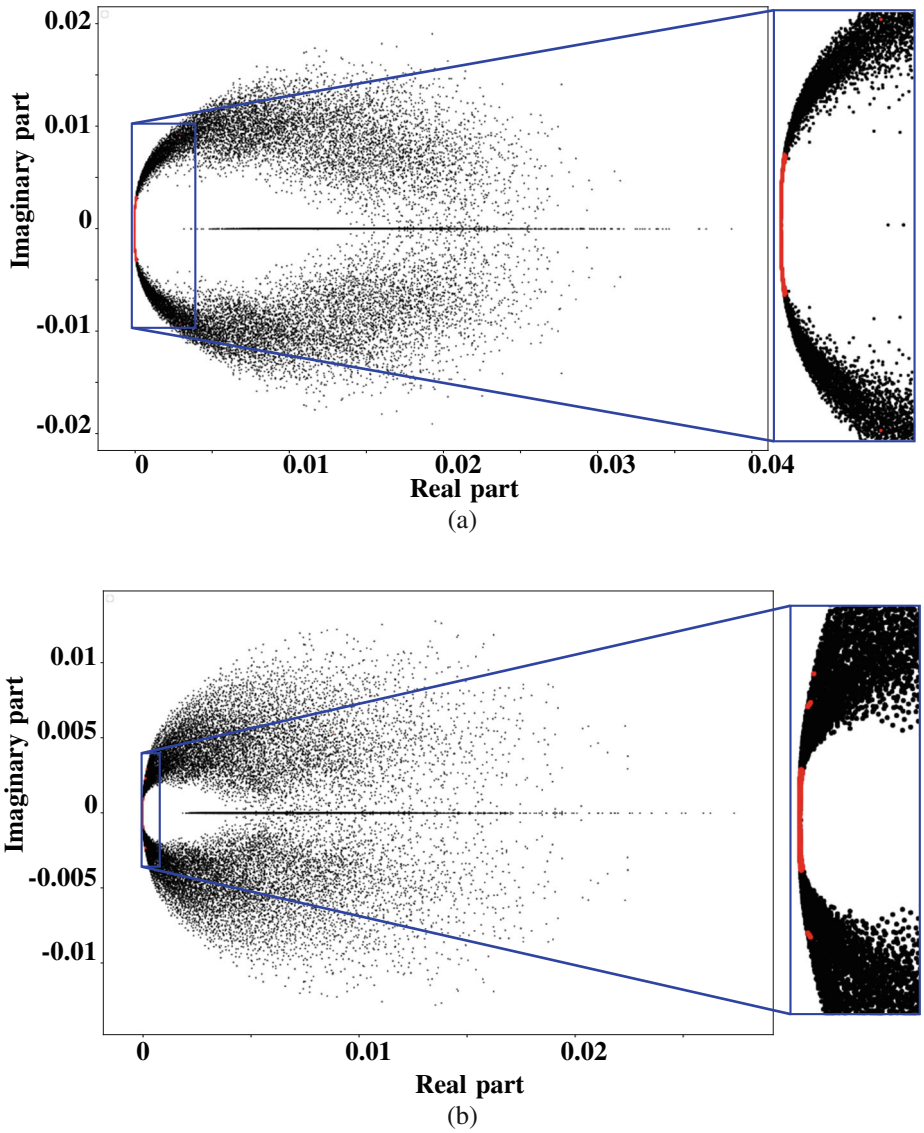

Fig. 3 Plot of the eigenvalues for the bathymetry of Hayes (2016) (**a**) and Ventura et al. (2012) (**b**). One can see the vertical symmetry of the plots corresponding to the fact that the complex eigenvalues always come with their complex conjugates. The resolved modes are colored in red. They all correspond to eigenvalues whose real part is really small (it is at most $\mathcal{O}(10^{-8})$)

$$\Leftrightarrow \mathbf{U}^p(x,y,t) = \mathrm{Re}\left\{\left[\mathbf{X}_\mathrm{r}^p(x,y)\cos(\omega t) - \mathbf{X}_\mathrm{i}^p(x,y)\sin(\omega t)\right] + j\left[\mathbf{X}_\mathrm{i}^p(x,y)\cos(\omega t) + \mathbf{X}_\mathrm{r}^p(x,y)\sin(\omega t)\right]\right\} \quad (8)$$

One can see that both the real and imaginary parts of the eigenvectors can contribute to the motion but there is a phase lag of $\frac{\pi}{2}$ between them.

The main drawback of the method used herein is that one mode is associated with each degree of freedom of the discrete equations, which results in an excessively large number of modes. Hence, both resolved and unresolved modes are obtained. The latter shorter normal modes have a wavelength that is too short to be well represented on the mesh (i.e. the mesh resolution is not significantly smaller than the wavelength) or represent numerical noise. These modes have to be distinguished a posteriori from the resolved modes and are disregarded.

3 Astronomical forcings

In this section, the astronomical forcings that could resonantly force Titan liquid bodies are listed. Tokano (2010) and Vincent et al. (2016) studied the tidal motion induced by Titan's obliquity and orbital eccentricity. However, other components of the tidally induced motion of the surface lakes and seas such as those induced by the sun, planets of the solar system, and Saturn's moons were neglected because they are much weaker (Sagan and Dermott 1982; Tokano 2010). Nevertheless, the forcings associated with these celestial bodies could, despite their small magnitude, excite a normal mode, resulting in a seiche through resonant amplification. Such phenomenon could generate a much larger liquid motion than the diurnal tidal motion. The most important of those tidal forcings arises through periodic perturbations in Titan's orbit induced by

the other moons of Saturn and celestial bodies of the solar system, resulting in a variation of Titan's gravitational force acting on the surface lakes and seas. Such variations were studied by, among others, Vienne and Duriez (1991, 1992, 1995), who took into account perturbations induced by the sun and by the other satellites of Saturn. The short-period variations predicted in these articles are listed in Table 1. Another way to detect a short-period variation of the forcing acting on Titan is to study its position as a function of time, which is available in the HORIZONS Web-Interface (https://ssd.jpl.nasa.gov/horizons.cgi). We took into account two reference points while studying the position of Titan: Saturn and the solar system barycenter. In both cases, we studied the evolution of the position with three different time steps: 1 day, 1 h, and 1 min. Focusing on the days/months before the first ISS observation (6th of June 2005), we did not detect any other periodic variations than those listed in Vienne and Duriez (1991, 1992, 1995). According to Hussmann et al. (2010), a resonance between Titan and Hyperion, which is not mentioned in Vienne and Duriez's (1991, 1992, 1995) list, can also be observed. This resonance has a period of 640 days and a libration amplitude of 36°.

4 Normal modes

A fundamental slosh is unlikely to develop as its period is much smaller than the period corresponding to the astronomical forcings listed in Table 1. Indeed, the latter have time scales of days while Merian's formula (Merian 1828) results in periods of 20.5678 h for the bathymetry of Hayes (2016) (whose mean depth is about 27.33 m) and 34.56 h for that of Ventura et al. (2012) (whose mean depth is about 9.68 m). Inverting Merian's formula to get the depth needed to create a wave slow enough to correspond to the periods of the astronomical forcings results in mean depths of less than 2 m (see Table 1), which does not correspond to the observations. Consequently, for a reasonable range of depths, none of the astronomical forcings periods corresponds to that of the fundamental slosh. Celestial bodies can also modify the length-of-day and polar motion of Titan due to the gravitational torque exerted on Titan and to the dynamic variations in the atmosphere (Coyette et al. 2018). Those rotation variations also influence the tides but are too small to affect significantly the tidal motion in Ontario Lacus. Moreover, the main atmospheric forcing is at annual, semi-anual, ter-annual, and 1/4 annual periods, which is too long to resonantly excite a barotropic mode. Therefore, they will not be able to generate any liquid motion on the surface lakes or seas, which is why they are not taken into account. Nevertheless, astronomical forcings could induce other resonance phenomena. In order to study such phenomena, the eigenmodes of Ontario Lacus are computed following the method of Bernard et al. (2008), as described in Section 2. As one can see in Figs. 4 and 5, the periods of the astronomical forcings (in red) do not match with any of the lake natural frequencies. Nevertheless, as there are uncertainties about the bathymetries and as the latter have an impact on the period and shape of the normal modes, we also studied the normal modes whose natural period is close (i.e. the difference is less than 2 h) to that of the forcings but they correspond to unresolved modes. Consequently, astronomical forcing is not expected to excite significant barotropic normal modes in Ontario Lacus.

Various types of normal modes can develop in a lake such as Ontario Lacus, depending on the relative importance of gravity, Titan's rotation speed, the depth of fluid column, and the gradient of it. The variation of the Coriolis parameter is negligible over the lake, which is why Rossby waves are unlikely to be observed. The size of the lake being much smaller than the external Rossby radius of deformation $\left(R = \frac{\sqrt{gh}}{|f|} \sim 700\ \text{km}\right)$, most inertia-gravity modes are little influenced by Titan's rotation. Nevertheless, some of the present numerical results point to the existence of normal modes bearing some similarities with Kelvin waves or topographic Rossby waves. These modes are localized along the shores of the lake, some of which can be associated with the area where local variations in the bathymetry are observed. Pure gravity waves are also obtained, mainly as sloshing modes. Some of them correspond to small oscillations in coves and bays while others correspond to the largest scale oscillations calculated by the present method. For instance, a normal mode appearing as a fundamental slosh was observed for both bathymetries (see the natural modes shown in Figs. 6d

Table 1 Short-period terms inducing perturbations of Titan orbital parameters larger than 10 km (a is the semi-major axis, λ is the mean longitude, and $z = e\exp(i\overline{\omega})$ (where e is the eccentricity and $\overline{\omega}$ is the periapsis longitude of Titan) represents the eccentricity and pericenter of Titan) due to the sun and other satellites of Saturn found in Vienne and Duriez (1991, 1992, 1995)

Orbital parameter	Period (in days)	Amplitude (km)	Depth (m)
a	6.303	20.5	0.505
a	3.304		1.838
λ	6.303		0.505
z	15.945	81.7	0.0789
z	4.518		0.983

The amplitudes of the associated perturbations (amplitudes smaller than 20 km are not specified) are shown in the third column and the mean depths required to develop a fundamental slosh are displayed in the fourth column

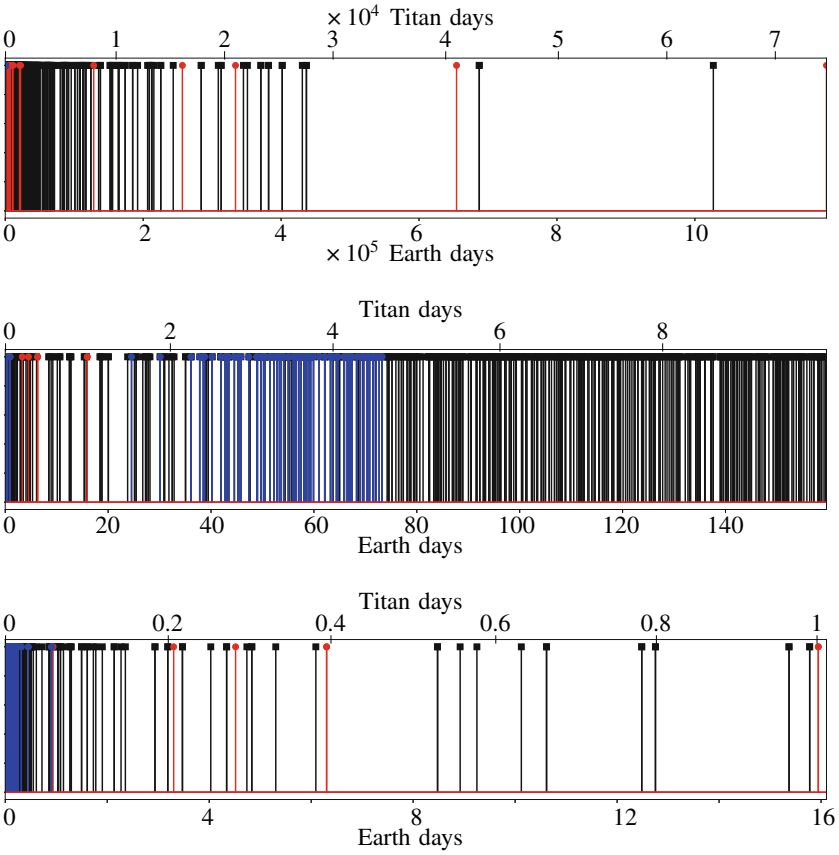

Fig. 4 Period of the normal modes of Ontario Lacus with the bathymetry of Hayes (2016) with focus from 0 to 10 Titan days and from 0 to 1 Titan day. The red and blue dots respectively correspond to the periods of the astronomical forcings and the natural periods of the modes associated with large-scale phenomena. The lower axis and the upper one of each subplot are graduated in earth days and Titan days, respectively

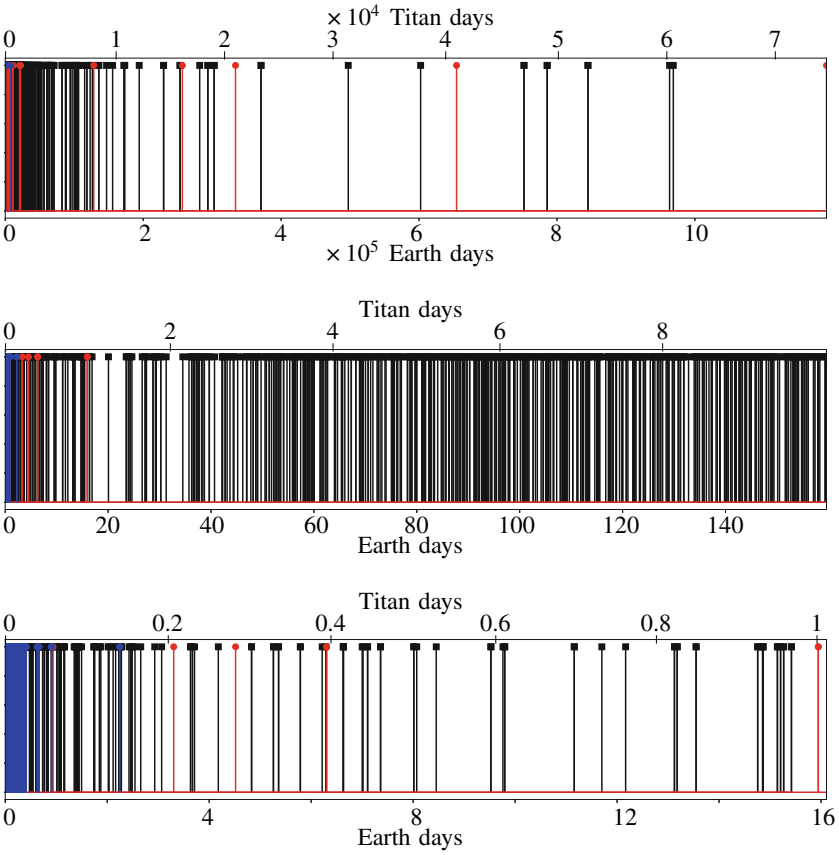

Fig. 5 Period of the normal modes of Ontario Lacus with the bathymetry of Ventura et al. (2012) with focus from 0 to 10 Titan days and from 0 to 1 Titan day. The red and blue dots respectively correspond to the periods of the astronomical forcings and the natural periods of the modes associated with large-scale phenomena. The lower axis and the upper one of each subplot are graduated in earth days and Titan days, respectively

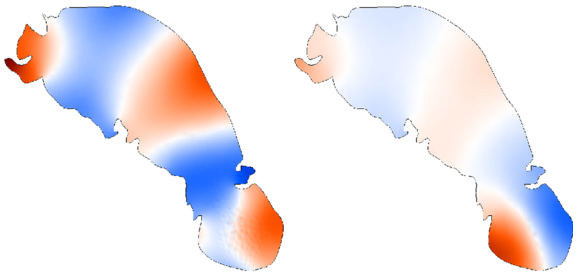

(a.1) Real part (a.2) Imaginary part

(a) $\omega = 2.37\ 10^{-8} + 3.23\ 10^{-4}\mathrm{j}\ \mathrm{s}^{-1}$

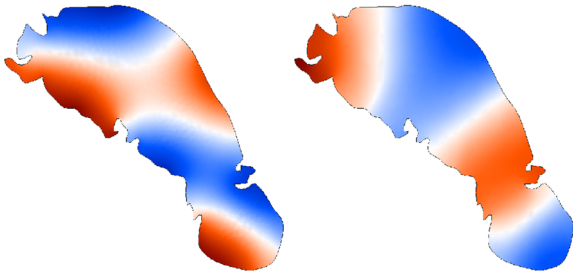

(b.1) Real part (b.2) Imaginary part

(b) $\omega = 7.65\ 10^{-9} + 2.31\ 10^{-4}\mathrm{j}\ \mathrm{s}^{-1}$

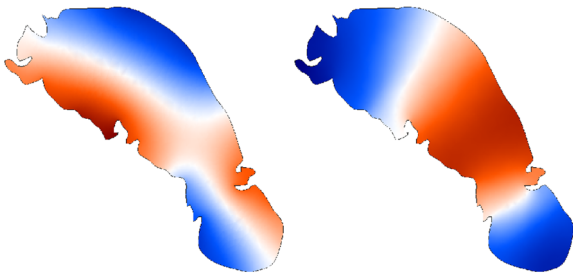

(c.1) Real part (c.2) Imaginary part

(c) $\omega = 3.55\ 10^{-9} + 1.61\ 10^{-4}\mathrm{j}\ \mathrm{s}^{-1}$

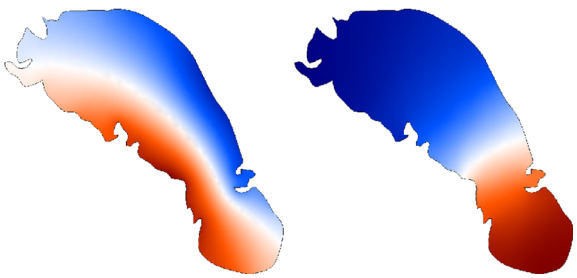

(d.1) Real part (d.2) Imaginary part

(d) $\omega = 6.52\ 10^{-10} + 8\ 10^{-5}\mathrm{j}\ \mathrm{s}^{-1}$

Fig. 6 Real and imaginary parts of the lake surface elevation normal modes of Ontario Lacus with the bathymetry of Hayes (2016). The red areas correspond to lake surface elevation above the reference level while the blue areas correspond to a lake surface elevation below the reference level. By definition, the eigenvectors are defined up to a multiplying constant. Consequently, their amplitude has no meaning while the spatial patterns do. The vectors are chosen so that the square of their Euclidean norm is 1. The (small) real part of the eigenvalues is due to the numerical dissipation of the numerical scheme used

and 7d). The natural periods of these modes respectively are 21.829 h and 53.876 h, which are close to the period predicted by Merian's formula (Merian 1828) (i.e. 20.5678 h and 34.56 h using the mean depth of the lake).

We only pay attention to the normal modes whose associate motion covers a significant portion of the lake. For both bathymetries, some of the normal modes (both their real and imaginary parts as explained in Section 2) correspond to large-scale variation of the lake surface elevation (see Figs. 6 and 7). They are associated with limited dissipation, as shown by the smallness of the real parts of the eigenvalues: the maximum is $\mathcal{O}(10^{-8})$ s^{-1} (see the eigenvalues associated with the modes in Figs. 6 and 7). The periods of the normal modes shown in Figs. 6 and 7 are respectively 5.397, 7.555, 10.839, and 21.829 h for the bathymetry of Hayes (2016) (Fig. 6) and 15.079, 15.904, 21.759, and 53.876 h for that of Ventura et al. (2012) (Fig. 7). Such periods are small with respect to a Titan day—which is about 382.74 h. Consequently, only phenomena characterized by a short time scale, such as atmospheric events, would be able to resonantly excite them. All of these modes correspond to sloshing modes and their natural period is close to the approximation given by Merian's formula (Merian 1828). Although the amplitude of the motion associated with the normal modes cannot be theoretically predicted, we conducted simulations under arbitrary wind conditions capable of exciting the natural modes shown in Figs. 6d and 7d. This allowed estimating the order of magnitude of the liquid motion associated with these normal modes. For a wind blowing along the main axis of the lake with a sinusoidal variation in time and a maximum speed[9] of 1 m/s, the amplitude of the free surface displacements of the ensuing modes does not exceed 0.2 m. This value should not be viewed as a true upper bound as stronger winds or other modes could be associated with a larger lake surface elevation.

5 Discussion

Due to the large discrepancy between the astronomical forcings periods and the natural periods of the lake, these forcings can be ruled out as a potential source of excitation of the normal modes. Indeed, although the natural periods critically depend on the bathymetry—as is shown by the variation between the two bathymetry maps implemented—the variations needed to get an overlap between the natural periods and those of the astronomical forcings are too large. For instance, the depth required to generate a fundamental slosh is not consistent with the observations (a simple

[9]The maximum wind speed is set to 1 m/s in accordance with existing data and atmospheric model results.

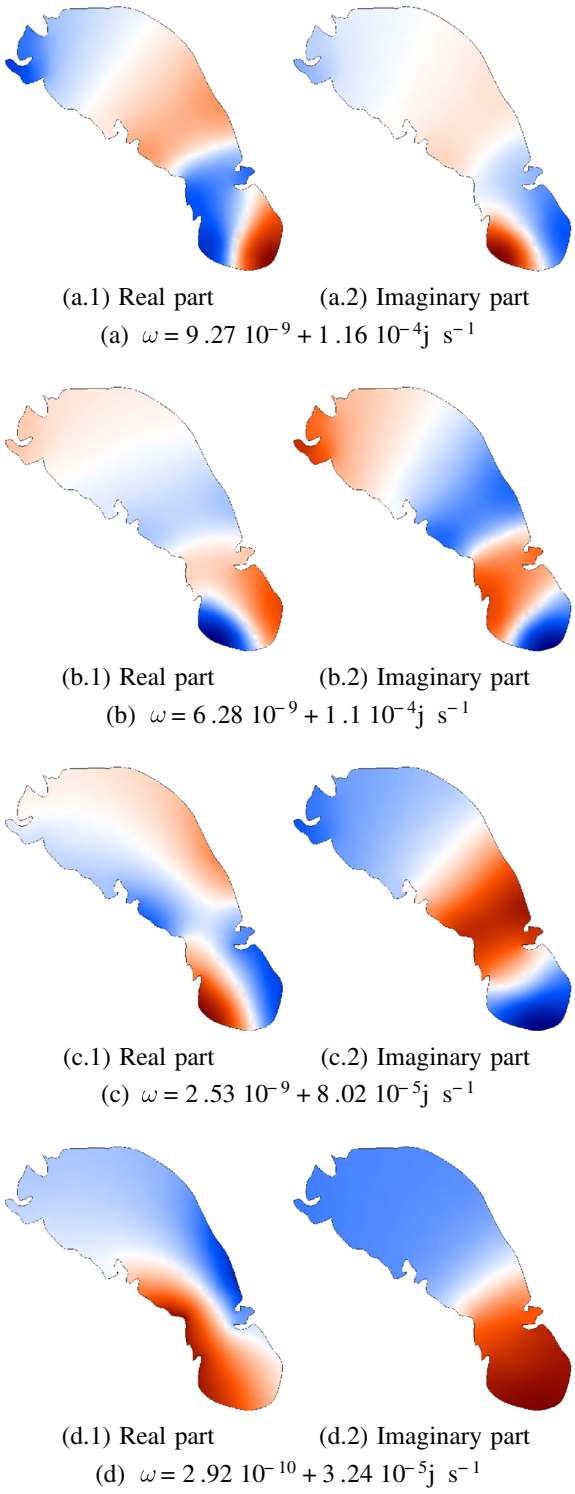

Fig. 7 Real and imaginary parts of the lake surface elevation normal modes of Ontario Lacus with the bathymetry of Ventura et al. (2012). The red areas correspond to lake surface elevation above the reference level while the blue areas correspond to a lake surface elevation below the reference level. By definition, the eigenvectors are defined up to a multiplying constant. Consequently, their amplitude has no meaning while the spatial patterns do. The vectors are chosen so that the square of their Euclidean norm is 1. The (small) real part of the eigenvalues is due to the numerical dissipation of the numerical scheme used

approximation predicts a depth of less than 2 m, which is inconsistent with Cassini radar images). Indirect rocking by the tidal response of the global subsurface ocean would rock the lake at the same frequency (i.e. the tidal frequency) and so is unlikely to generate resonant amplification in the lakes. A resonant subsurface ocean could rock at frequencies smaller than the tidal frequency and hence resonantly force the lake, but the liquid motion in the ocean widely varies with the parameter assumptions and there is no observations of such a phenomenon. The inability of astronomical forcings to resonantly force a normal mode is given support by the observations of Cassini. Although shoreline variations were observed, they are claimed to be due to methane evaporation and/or infiltration. Indeed, the 2005 shoreline lies beyond the 2009 coastline except in the northwest corner but this could not compensate the negative sea surface elevation elsewhere in the lake. Furthermore, sloshing conserves volume and the slope in the fluid induced by an almost uniform retreat should be detectable by SAR.

Atmospheric forcing such as the wind could also resonantly force the normal modes of the lake. Annual and diurnal wind variations predicted by the global circulation models (GCM) are slow, at most 2 m/s, but thanks to the density difference between Titan's atmosphere and the lake liquid, they can generate significant liquid motion in the northern seas (see Tokano and Lorenz 2015). However, they are unlikely to resonantly force the lake due to their diurnal period. Shorter period traveling waves taking place in Titan's atmosphere are more likely to excite a natural mode in the lake. Such waves were predicted by, among others, Lebonnois et al. (2012). The frequencies of the dominant groups of waves are 5–7 cycles/Titan day and 10–12 cycles/Titan day (Lebonnois et al. 2012). The magnitude of the zonal and meridional wind associated with the traveling waves strongly varies with the altitude: from less than 1 m/s in the lower troposphere to more than 10 m/s in the stratosphere (see Figs. 15 and 16 of Lebonnois et al. 2012). Hence, the magnitude of the forcing acting on the lake, which is a function of the wind velocity 10 m above the lake surface, should be very small[10] despite the significant density difference between the atmosphere and the lake. If the resulting forcing is strong enough to excite the natural modes, it would result in localized lake surface motion near the shore. The amplitude of such motions, although presumably small, could be significant as compared with the tidal range. Mitchell et al. (2011) also predicted eastward propagating equatorially trapped Kelvin waves whose period and phase speed at the equator are about 8 days and 12 m/s, respectively, and a slow

[10] According to Lebonnois et al. (2012), the wind velocity associated with theses waves is less than 0.4 m/s near the surface (see Figs. 15 and 16 (a) of Lebonnois et al. 2012).

westward propagating mode whose period and phase speed are about 100 days and 1 m/s, respectively. Those wave periods are much larger than the lake's natural periods. Furthermore, the lake is located at high latitudes, far from the equator. Hence, interactions between these waves and Ontario Lacus are unlikely. One-time events such as storms could result in stronger winds more likely to generate large amplitude liquid motion. Using a mesoscale model, Charnay et al. (2015) predicted that methane storms are accompanied by eastward gust front above the surface. The wind speed in these fronts can reach up to 10 m/s, which would be more than enough to resonantly force the normal modes of Ontario Lacus, depending on the gusts' spatial and temporal patterns. Such storms are characterized by the presence of convective clouds. The convection cells associated with such clouds have been reported as able to generate significant seiches on earth (see, for instance, the seiche in Rotterdam harbor described by De Jong and Battjes 2004). Rodriguez et al. (2013) and Turtle et al. (2018) have listed the cloud observations on Titan for over 13 years. Observations prior to the arrival of Cassini were made by means of earth-based instruments until Cassini's visual and infrared mapping spectrometer (VIMS) and Imaging Science Subsystem (ISS) could be used. Outbursts of large clouds at Titan's southern pole were observed almost continuously by earth-based campaigns from December 2001 to December 2005 (Rodriguez et al. 2013). Afterwards, cloud activity in the south pole began to decline and the stormy activity disappeared after 2008 (Turtle et al. 2018). Consequently, during the period of large cloud outbursts, strong winds able to resonantly force the lake could have occurred in the vicinity of Ontario Lacus. Unfortunately, the observations of Ontario Lacus do not show lake surface elevation corresponding to the normal modes.

The lake bathymetry does influence the period and shape of the natural modes. The significant lake level change observed between 2005 and 2009 by Hayes et al. (2011) and Turtle et al. (2011) would, for instance, result in variations of the normal modes' shape and period. Hayes et al. (2011) predicted a lake level change of about 4 m over a period of 4 years. While studying the impact of such a variation on all the normal modes would be complicated due to the absence of a bathymetry and coastline corresponding to the 2005 data, it is interesting to assess whether its impact on the normal modes is significant. To this end, Merian's formula (Merian 1828) is resorted to to compute the period of a fundamental slosh within the lake for a bathymetry increased by 4 m (without modifying the coastline). It results in decreasing the fundamental slosh's period by 1.36 h and 5.49 h for Hayes (2016)'s and Ventura et al. (2012)'s bathymetries, respectively. The latter being more shallow, the natural periods are more sensitive to the lake level variation. Although significant, these differences are smaller than those observed between the normal periods for both bathymetries. Indeed, while the shape of the natural modes remains similar, the periods of similar modes can be significantly different, which can be explained by the significant depth variations (up to 38 m) between the bathymetries. The shape of a natural mode can be considered rather insensitive to the bathymetry but they can change with the shoreline. Consequently, if the lake is filled with methane precipitation or if another strong evaporation period took place, the shape and period of the natural mode would change.

The normal modes of Ontario Lacus, if excited to a sufficiently large amplitude, could be observed by future missions. Among the proposals discussed in the literature, some are better suited for this purpose than others. An orbiter such as Oceanus (see Sotin et al. 2017) could detect modes whose period is at least twice the sampling period, in accordance with the Nyquist-Shannon sampling theorem. The main limitation would be related to the amplitude that can be measured by a spacecraft instrument. The amplitude of the liquid motion associated to the normal modes is expected to be of the order of 10^{-1} m under astronomic forcing and no stormy wind conditions. Stormy wind conditions would increase the amplitude but the cloud outbursts associated with such an event could prevent observations, depending on the instrument used. A lake probe with an orbiter (such as the E2T, see Mitri et al. 2014), a drifted capsule (similar to the TiME proposed for Ligeia Mare, see Lorenz et al. 2012), a lander (such as the Dragonfly rotorcraft Lorenz et al. 2018), or a submarine (such as the Titan sub proposed for Kraken Mare, see Hartwig et al. 2016) would be better suited to observe natural modes without discrimination as to their period. Observations from a probe would be conditioned by its landing site and its ability to observe lake surface elevation. If it sinks in the lake, it could act as a tidal gauge and would be able to detect all the normal modes excited as well as the tide at a specific location. On earth, tidal gauges are accurate up to 10^{-3} m. Acoustic/radar tidal gauges rely on wave propagation within the liquid while the mean density and the atmospheric pressure are required to use a pressure tidal gauge. If the probe lands near the shores, it could use a laser rangefinder but it would have to use a wavelength to which the liquid is opaque. A lander would have the same advantages but would be able to study several areas. A floating platform or a surfaced submarine could also perform similar measurements and would offer the additional benefit of being able to conduct measurements at various locations. Using a sonar or a laser rangefinder would allow to accurately measure the lake surface elevation as a function of time. Such platforms would still be better suited if they were motorized as their localization and their spatial

evolution could be forced instead of being driven by the fluid flow or wind stress.

6 Conclusion

Ontario Lacus was the focus of various studies since its discovery. Although many aspects of the lake were studied, the natural modes were only briefly investigated by Tokano (2010). In this paper, we numerically predicted the normal modes of the lake for the two bathymetries available in the literature. We used the method of Bernard et al. (2008) to compute the modes of the lake as this method allows us to use unstructured meshes to discretize the domain; hence, the spatial resolution can be increased to capture the coastline while keeping a reasonable computer cost.

The frequency of the tidal forces is too small to excite the (barotropic) normal modes, and a slosh between the northern and southern shores would require a fast propagation speed corresponding to a mean lake depth not met by the observations. Such low-frequency forcings could more easily resonantly force the baroclinic normal modes, but investigating this phenomenon requires unavailable information about the lake stratification. On the other hand, wind forcing could likely coincide with the resonant frequencies but it would require specific events such as a storm to generate wind strong enough to excite the normal modes significantly enough to be observable by an orbiter. The large-scale normal modes predicted could be observed by an orbiter if they were excited, but it was not the case during the Cassini observation.

Funding information Computational resources were provided by the Consortium des Équipements de Calcul Intensif (CÉCI), funded by the Belgian Fund for Scientific Research (F.R.S.-FNRS) under Grant No. 2.5020.11. Eric DELEERSNIJDER is an honorary Research associate with the F.R.S.-FNRS. This research is funded by the Belgian PRODEX, managed by the ESA, in collaboration with the Belgian Federal Science Policy Office.

References

Aharonson O, Hayes AG, Lunine JI, Lorenz RD, Allison MD, Elachi C (2009) An asymmetric distribution of lakes on Titan as a possible consequence of orbital forcing. Nat Geosci 2(12):851–854. https://doi.org/10.1038/ngeo698

Atreya SK, Adams EY, Niemann HB, Demick-Montelara JE, Owen TC, Fulchignoni M, Ferri F, Wilson EH (2006) Titan's methane cycle. Planet Space Sci 54(12):1177–1187. https://doi.org/10.1016/j.pss.2006.05.028

Baretta-Bekker HJ, Duursma EK, Kuipers BR (1998) Encyclopedia of marine sciences. Springer Science & Business Media

Bernard PE, Deleersnijder E, Legat V, Remacle JF (2008) Dispersion analysis of discontinuous Galerkin schemes applied to Poincaré, Kelvin and Rossby waves. J Sci Comput 34(1):26–47. https://doi.org/10.1007/s10915-007-9156-6

Brown RH, Soderblom LA, Soderblom JM, Clark RN, Jaumann R, Barnes JW, Sotin C, Buratti B, Baines KH, Nicholson PD (2008) The identification of liquid ethane in Titan's Ontario Lacus. Nature 454(7204):607–610. https://doi.org/10.1038/nature07100

Charnay B, Barth E, Rafkin S, Narteau C, Lebonnois S, Rodriguez S, Du Pont SC, Lucas A (2015) Methane storms as a driver of Titan's dune orientation. Nat Geosci 8(5):362. https://doi.org/10.1038/ngeo2406

Cordier D, Mousis O, Lunine JI, Lavvas P, Vuitton V (2009) An estimate of the chemical composition of Titan's lakes. Astrophys J Lett 707(2):L128. https://doi.org/10.1088/0004-637X/707/2/L128

Cornet T, Bourgeois O, Le Mouélic S, Rodriguez S, Gonzalez TL, Sotin C, Tobie G, Fleurant C, Barnes J, Brown R et al (2012) Geomorphological significance of Ontario Lacus on Titan: integrated interpretation of cassini VIMS, ISS and RADAR data and comparison with the Etosha Pan (Namibia). Icarus 218(2):788–806. https://doi.org/10.1016/j.icarus.2012.01.013

Coyette A, Baland RM, Van Hoolst T (2018) Variations in rotation rate and polar motion of a non-hydrostatic Titan. Icarus 307:83–105. https://doi.org/10.1016/j.icarus.2018.02.003

De Jong M, Battjes J (2004) Low-frequency sea waves generated by atmospheric convection cells. J Geophys Res-Oceans 109:C1. https://doi.org/10.1029/2003JC001931

Dermott SF, Sagan C (1995) Tidal effects of disconnected hydrocarbon seas on Titan. Nature 374(6519):238–240. https://doi.org/10.1038/374238a0

Geuzaine C, Remacle JF (2009) Gmsh: a 3-d finite element mesh generator with built-in pre-and post-processing facilities. Int J Numer Methods Eng 79(11):1309–1331. https://doi.org/10.1002/nme.2579

Hartwig JW, Colozza A, Lorenz RD, Oleson S, Landis G, Schmitz P, Paul M, Walsh J (2016) Exploring the depths of Kraken Mare–power, thermal analysis, and ballast control for the Saturn Titan submarine. Cryogenics 74:31–46. https://doi.org/10.1016/j.cryogenics.2015.09.009

Hayes AG (2016) The lakes and seas of Titan. Annu Rev Earth Pl Sc, 44. https://doi.org/10.1146/annurev-earth-060115-012247

Hayes AG, Aharonson O, Callahan P, Elachi C, Gim Y, Kirk RL, Lewis K, Lopes R, Lorenz RD, Lunine JI et al (2008) Hydrocarbon lakes on Titan: distribution and interaction with a porous regolith. Geophys Res Lett 35:9. https://doi.org/10.1029/2008GL033409

Hayes AG, Wolf AS, Aharonson O, Zebker H, Lorenz RD, Kirk RL, Paillou P, Lunine JI, Wye L, Callahan P et al (2010) Bathymetry and absorptivity of Titan's Ontario Lacus. J Geophys Res-Planet 115:E9. https://doi.org/10.1029/2009JE003557

Hayes AG, Aharonson O, Lunine JI, Kirk RL, Zebker HA, Wye LC, Lorenz RD, Turtle EP, Paillou P, Mitri G et al (2011) Transient surface liquid in Titan's polar regions from Cassini. Icarus 211(1):655–671. https://doi.org/10.1029/2009JE003557

Hayes AG, Lorenz RD, Lunine JI (2018) A post-cassini view of Titan's methane-based hydrologic cycle. Nat Geosci 11:306–313. https://doi.org/10.1038/s41561-018-0103-y

Hussmann H, Choblet G, Lainey V, Matson DL, Sotin C, Tobie G, Van Hoolst T (2010) Implications of rotation, orbital states, energy sources, and heat transport for internal processes in icy satellites. Space Sci Rev 153(1–4):317–348. https://doi.org/10.1007/s11214-010-9636-0

Jones E, Oliphant T, Peterson P et al (2001) SciPy: open source scientific tools for Python. http://www.scipy.org/ [Online; accessed May 2018]

Lebonnois S, Burgalat J, Rannou P, Charnay B (2012) Titan global climate model: a new 3-dimensional version of the IPSL Titan GCM. Icarus 218(1):707–722. https://doi.org/10.1016/j.icarus.2011.11.032

Lorenz RD (1994) Crater lakes on Titan: rings, horseshoes and bullseyes. Planet Space Sci 42(1):1–4. https://doi.org/10.1016/0032-0633(94)90134-1

Lorenz RD, Tokano T, Newman CE (2012) Winds and tides of Ligeia Mare, with application to the drift of the proposed time TiME (Titan Mare Explorer) capsule. Planet Space Sci 60(1):72–85. https://doi.org/10.1016/j.pss.2010.12.009

Lorenz RD, Turtle EP, Barnes JW, Trainer MG, Adams DS, Hibbard KE, Sheldon CZ, Zacny K, Peplowski PN, Lawrence DJ et al (2018) Dragonfly: a rotorcraft lander concept for scientific exploration at Titan. Johns Hopkins APL Technical Digest

Lunine JI, Hayes A, Aharonson O, Mitri G, Lorenz R, Stofan E, Wall S, Elachi C, Team CR et al (2009) Evidence for liquid in Ontario Lacus (Titan) from Cassini-observed changes. In: AAS/Division for planetary sciences meeting abstracts# 41, vol 41

Mastrogiuseppe M, Poggiali V, Hayes A, Lorenz R, Lunine J, Picardi G, Seu R, Flamini E, Mitri G, Notarnicola C et al (2014) The bathymetry of a Titan sea. Geophys Res Lett 41(5):1432–1437. https://doi.org/10.1002/2013GL058618

Mastrogiuseppe M, Poggiali V, Hayes A, Lorenz R, Lunine JI, Hofgartner J (2016) Radar sounding using the Cassini altimeter: waveform modeling and Monte Carlo approach for data inversion of observations of Titan's seas. IEEE T Geosci Remote 54(10):5646–5656. https://doi.org/10.1109/TGRS.2016.2563426

Mastrogiuseppe M, Hayes AG, Poggiali V, Lunine JI, Lorenz R, Seu R, Le Gall A, Notarnicola C, Mitchell KL, Malaska M et al (2018) Bathymetry and composition of Titan's Ontario Lacus derived from Monte Carlo-based waveform inversion of Cassini RADAR altimetry data. Icarus 300:203–209. https://doi.org/10.1016/j.icarus.2017.09.009

Merian J (1828) Ueber die bewegung tropfbarer flüssigkeiten in gefässen [on the motion of drippable liquids in containers]. PhD thesis PhD thesis. Basel, Schweighauser

Mitchell JL, Ádámkovics M, Caballero R, Turtle EP (2011) Locally enhanced precipitation organized by planetary-scale waves on Titan. Nat Geosci 4:589–592. https://doi.org/10.1038/ngeo1219

Mitri G, Coustenis A, Fanchini G, Hayes AG, Iess L, Khurana K, Lebreton JP, Lopes RM, Lorenz RD, Meriggiola R et al (2014) The exploration of Titan with an orbiter and a lake probe. Planet Space Sci 104:78–92. https://doi.org/10.1016/j.pss.2014.07.009

Porco CC, West RA, Squyres S, Mcewen A, Thomas P, Murray CD, Delgenio A, Ingersoll AP, Johnson TV, Neukum G et al (2004) Cassini imaging science: instrument characteristics and anticipated scientific investigations at Saturn. Space Sci Rev 115(1-4):363–497. https://doi.org/10.1007/s11214-004-1456-7

Rodriguez S, Le Mouélic S, Rannou P, Sotin C, Brown R (2013) Six years of continuous observation of Titan cloud activity with Cassini/VIMS. In: SF2A-2013: Proceedings of the annual meeting of the French society of astronomy and astrophysics, pp 71–74

Sagan C, Dermott SF (1982) The tide in the seas of Titan. Nature 300(5894):731–733. https://doi.org/10.1038/300731a0

Sauter S, Wittum G (1992) A multigrid method for the computation of eigenmodes of closed water basins. Impact Comput Sci Eng 4(2):124–152. https://doi.org/10.1016/0899-8248(92)90019-5

Sotin C, Hayes AG, Malaska MJ, Nimmo F, Trainer M, Mastrogiuseppe M, Soderblom JM, Tortora P, Hofgartner JD, Aharonson O, Barnes JW, Hodyss R, Iess L, Kirk RL, Lavvas P, Lorenz RD, Lunine JI, Mazarico E, McEwen AS, Neish C, Nixon CA, Turtle EP, Vuitton V, Yelle R (2017) Oceanus: a new frontiers orbiter to study Titan's potential habitability. In: 48th Lunar and planetary science conference, lunar and planetary science conference, vol 48, p 2306

Stofan ER, Elachi C, Lunine JI, Lorenz RD, Stiles B, Mitchell KL, Ostro S, Soderblom L, Wood C, Zebker H et al (2007) The lakes of Titan. Nature 445(7123):61–64. https://doi.org/10.1038/nature05438

Tokano T (2010) Simulation of tides in hydrocarbon lakes on Saturn's moon Titan. Ocean Dyn 60(4):803–817. https://doi.org/10.1007/s10236-010-0285-3

Tokano T, Lorenz RD (2015) Wind-driven circulation in Titan's seas. J Geophys Res-Planet 120(1):20–33. https://doi.org/10.1002/2014JE004751

Tokano T, Lorenz RD, Van Hoolst T (2014) Numerical simulation of tides and oceanic angular momentum of Titan's hydrocarbon seas. Icarus 242:188–201. https://doi.org/10.1016/j.icarus.2014.08.021

Turtle E, Perry J, Barbara J, Del Genio A, Rodriguez S, Le Mouélic S, Sotin C, Lora J, Faulk S, Corlies P et al (2018) Titan's meteorology over the Cassini mission: evidence for extensive subsurface methane reservoirs. Geophys Res Lett 45(11):5320–5328. https://doi.org/10.1029/2018GL078170

Turtle EP, Perry JE, Hayes AG, McEwen AS (2011) Shoreline retreat at Titan's Ontario Lacus and Arrakis Planitia from Cassini imaging science subsystem observations. Icarus 212(2):957–959. https://doi.org/10.1016/j.icarus.2011.02.005

Ventura B, Notarnicola C, Casarano D, Posa F, Hayes AG, Wye L (2012) Electromagnetic models and inversion techniques for Titan's Ontario Lacus depth estimation from Cassini RADAR data. Icarus 221(2):960–969. https://doi.org/10.1016/j.icarus.2012.09.011

Vienne A, Duriez L (1991) A general theory of motion for the eight major satellites of Saturn. II-Short-period perturbations. Astron Astrophys 246:619–633

Vienne A, Duriez L (1992) A general theory of motion for the eight major satellites of Saturn. III-Long-period perturbations. Astron Astrophys 257:331–352

Vienne A, Duriez L (1995) TASS1 6: Ephemerides of the major Saturnian satellites. Astron Astrophys 297:588

Vincent D, Karatekin Ö, Vallaeys V, Hayes AG, Mastrogiuseppe M, Notarnicola C, Dehant V, Deleersnijder E (2016) Numerical study of tides in Ontario Lacus, a hydrocarbon lake on the surface of the Saturnian moon Titan. Ocean Dyn 66(4):461–482. https://doi.org/10.1007/s10236-016-0926-2

Vincent D, Karatekin Ö, Lambrechts J, Lorenz RD, Dehant V, Deleersnijder É (2018) A numerical study of tides in Titan's northern seas, Kraken and Ligeia Maria. Icarus 310:105–126. https://doi.org/10.1016/j.icarus.2017.12.018

Wall S, Hayes AG, Bristow C, Lorenz RD, Stofan ER, Lunine JI, Le Gall A, Janssen M, Lopes R, Wye L et al (2010) Active shoreline of Ontario Lacus, Titan: a morphological study of the lake and its surroundings. Geophys Res Lett 37(5):L05, 202. https://doi.org/10.1029/2009GL041821

Webb D (2013) On the shelf resonances of the English Channel and Irish Sea. Ocean Sci 9(4):731–744. https://doi.org/10.5194/os-9-731-2013